



Scholars Research Library

Der Pharma Chemica, 2015, 7(1):212-223
(<http://derpharmachemica.com/archive.html>)



ISSN 0975-413X
CODEN (USA): PCHHAX

The influence of variations in polyethylene glycol molecular weight on the morphology, spectroscopic and thermal properties of flower-like SnO₂ nanorod bundles prepared via solvothermal technique

J. Jayashainy and P. Sagayaraj*

Department of Physics, Loyola College (Autonomous), Chennai, India

ABSTRACT

Uniform flower-like SnO₂ nanoarchitectures built by numerous one-dimensional nanorod bundles are fabricated through a cost effective solvothermal technique by employing Polyethylene Glycol (PEG) as a structure directing agent. The variations in the molecular weight of PEG are found to influence the size, morphology, growth rate and yield of SnO₂ nanorods. The crystal structure, morphology and the elemental composition of the resulting nanorods are characterized by powder X-ray diffraction (XRD), Field Emission Scanning Electron Microscopy (FESEM), High-Resolution Transmission Electron Microscopy (HRTEM) and Energy Dispersive X-ray analysis (EDX). The optical property of the product has been explored by UV-Visible absorption, Fourier Transform Infrared (FT-IR) and FT-Raman spectroscopic techniques. FT-Raman peaks confirm the tetragonal rutile phase of SnO₂. Thermogravimetric analysis has been performed to determine the thermal stability of the as-prepared samples.

Keywords: Semiconductor metal oxides; Nanorods; Solvothermal process; Electron microscopy; Spectroscopy; Thermal analysis.

INTRODUCTION

Among the various low dimensional nanostructures reported, one-dimensional (1D) nanostructures of semiconductors have been an interesting area of research owing to their unique properties and novel applications in technological fields. As an important metal oxide semiconductor, tin oxide (SnO₂) with its wide band gap energy ($E_g = 3.6$ eV) is a potential material for application in chemical sensors, lithium ion batteries, solar cells, photocatalysts [1], nanofiltration membranes and electrochemical windows [2]. There are several articles that deal with the fabrication of 1D SnO₂ nanoarchitectures with well defined morphologies such as nanoribbon, nanowires, nanorods, nanotubes and nanobelts [3] employing variety of techniques including, template induced growth, pulsed laser deposition [4], plasma treatment [5], sonochemical, thermal evaporation, sol-gel and microemulsion process [6]. Though, each of these methods have been developed successfully to achieve 1D nanostructures, the complex process involved and the control over the morphology with tunable dimension are the main obstacles for achieving the uniform performances in nanodevices [5]. It is well known that the gas sensing properties of materials are greatly affected by their size and morphology. Flower-like SnO₂ nanostructures with well controlled dimensionality exhibited high response to CO, which makes it a competitive candidate for application in CO detecting [7]. Solvothermal method has been investigated to be a scalable and economical approach for the successful preparation to generate 1D nanostructures [8]. 1D SnO₂ nanomaterial with uniform structure can be produced by adding organic compounds like; polymers and surfactants into the reaction system. Different structure directing agents such as

cetyltrimethyl ammonium bromide (CTAB), hydrazine hydrate, hexylphosphonic acid (HPA), triocylphosphonic acid (TOPO), sodium dodecyl sulphate, polyethylene glycol (PEG) and poly (vinyl pyrrolidone) were successfully used to direct or control the anisotropic growth of SnO₂ nanostructures [8][9]. Lin Tan et al. have reported on the hydrothermal synthesis of SnO₂ involving the reaction of tin chloride and sodium dodecyl sulphate (SDS) at 200 °C in hexanol and heptanes, to obtain 1D rod-like nanostructures with a diameter of 20-40 nm and length of 100-300 nm [10]. Though the experimental route is straightforward and readily reproducible, the usage of organic reagents in the growth process significantly leads to negative effects on human health and environment [11]. It is therefore desirable to fabricate SnO₂ nanorods without using poisonous structure directing agent. The nonionic PEG was investigated to be one of the less toxic structure directing agents used in the cleaning of exhaust air and gas streams from industrial production plants owing to its favorable properties, such as low vapor pressure, high chemical stability and low melting point [12]. Xiaoming Zhou et al. optimized the PEG (M_w=400) dosage and investigated its effect in controlling the morphology and further compared it with the flower-like SnO₂ nanorods that were synthesized without PEG. Ya-Xia Yin et al. observed that on increasing the concentration of PEG from 40 to 60%, SnO₂ nanowires with enhanced length ranging between 4 and 5 μm are formed. On further increasing the concentration to 85%, the nanowires showed an increase in length to almost 40 μm [13]. Thus PEG plays a crucial role in both inducing the formation of nuclei and directing the growth of the crystals [14]. A scan on literature suggests that there are only limited number of articles that deal with the fabrication of PEG directed SnO₂ nanostructures, especially; in the form of flower-like nanorod bundles. Hence, there is a scope for further research to explore the effect of change in PEG molecular weight on the morphological and physical properties of SnO₂.

In this work, attempts have been made to establish the influence of variations in the molecular weight of PEG on the size dependent optical, structural and morphological characteristics of SnO₂ nanostructures. A simple, yet efficient solvothermal technique is employed for the preparation of 1D SnO₂ nanostructures under the influence of polyethylene glycol (PEG) of 3 different molecular weights i.e PEG 300, 400 and 600 at a relatively low temperature of 200°C. The less toxic nature of PEG coupled with the simple and straight forward solvothermal process employed in our experiments to fabricate reasonably good quality SnO₂ nanorods is the key focus of this article. The growth mechanism, effect of pH, volume ratio between surfactant and water, influence of temperature and time are also investigated in detail.

MATERIALS AND METHODS

2.1 Chemicals used

Five-hydrated tin tetrachloride (SnCl₄·5H₂O) was purchased from Sigma Aldrich, sodium hydroxide (NaOH), ethanol, Polyethylene glycol (HO(C₂H₄O)_nH) were purchased from Merck Specialties Pvt. Ltd., Mumbai. All the chemicals were used as received without further purification.

2.2 Material Synthesis

In a typical synthesis procedure, 1.5 mmol of 5-hydrated tin tetrachloride (SnCl₄·5H₂O) was added into a 10 ml of sodium hydroxide (0.302 g) solution under stirring. After about 5 min, 5 ml of polyethylene glycol (PEG, M_w=300) was added into the above solution with the constant stirring for about one hour. After which, when 10 ml of absolute ethanol was added it resulted in a white translucent suspended solution. The pH was noted to be 12 and the solution was then transferred into a Teflon-lined stainless steel autoclave. It was kept inside the furnace at 200°C and after 24 h of heat treatment; the autoclave was cooled to room temperature naturally. The resulting white precipitate was collected by centrifugation, and washed several times with distilled water and ethanol respectively, followed by vacuum drying at 80 °C for 6 h. Similar procedure was adopted for the preparation of two more samples by replacing PEG 300 with the higher molecular weight PEG 400 and PEG 600. When the synthesis was carried out with PEG 400 and PEG 600, the other experimental conditions remained unchanged.

2.3 Characterization techniques

The X-ray diffraction patterns of the as-prepared nanoparticles were investigated by a GE - XRD 3003 TT using monochromatic nickel filtered CuK_α (λ=1.5406 Å) radiation. Field Emission Scanning electron microscope (FESEM) was employed for morphological study with a CARL ZEISS SUPRA 55 operated at an accelerating voltage of 10 kV and 20 kV. It is also attached with Energy Dispersive X-ray analyzer (EDAX) for elemental analysis. The optical properties were studied using absorption spectrum in the spectral region of 200 to 800 nm by employing a T90+ UV/Vis Spectrophotometer. FT-RAMAN spectra were recorded with a BRUKER RFS in a spectral range of 50-4000 cm⁻¹ with a Nd:YAG as laser source having laser wavelength of 1064 nm. Shimadzu

IRAFFINITY-1 FT-IR instrument was employed for recording the FT-IR spectrum. Brunauer-Emmett-Teller (BET) surface area and porosity of the nanopowder were measured by employing MICROMERITICS ASAP 2020 porosimeter. Thermogravimetric (TG) and Differential Thermogravimetric Analysis (DTA) were performed on a TGA7 (Perkin Elmer), under nitrogen atmosphere.

RESULTS AND DISCUSSION

3.1 Powder XRD analysis

The X-ray diffraction (XRD) patterns of the three samples of PEG assisted SnO₂ nanostructures are shown in Fig. 1(a-c). The diffraction peaks are in accordance with the tetragonal rutile structure of SnO₂, revealing the selective phase formation and peak corresponding to any kind of impurity is not observed [15]. The difference in relative intensities of (101) peak from that of the bulk material, reveals the anisotropic growth behavior of the products [16]. However, the obvious preferential texturing cannot be found from the comparison between the experimental data and JCPDS card (77-0452) [10]. All the obtained samples show the SnO₂ crystal phase, with peaks becoming broader from (a) to (c), which is believed to have resulted from the size effect of the crystals [17]. Though, it is obvious from the earlier work that the XRD pattern showed increased crystallinity with increased intensity at higher pH values [6], there is a drastic decrease in the intensity of the peaks obtained for PEG 600 which might be due to the poor growth of the nuclei when critical concentration of the spontaneous nucleation was reached [18].

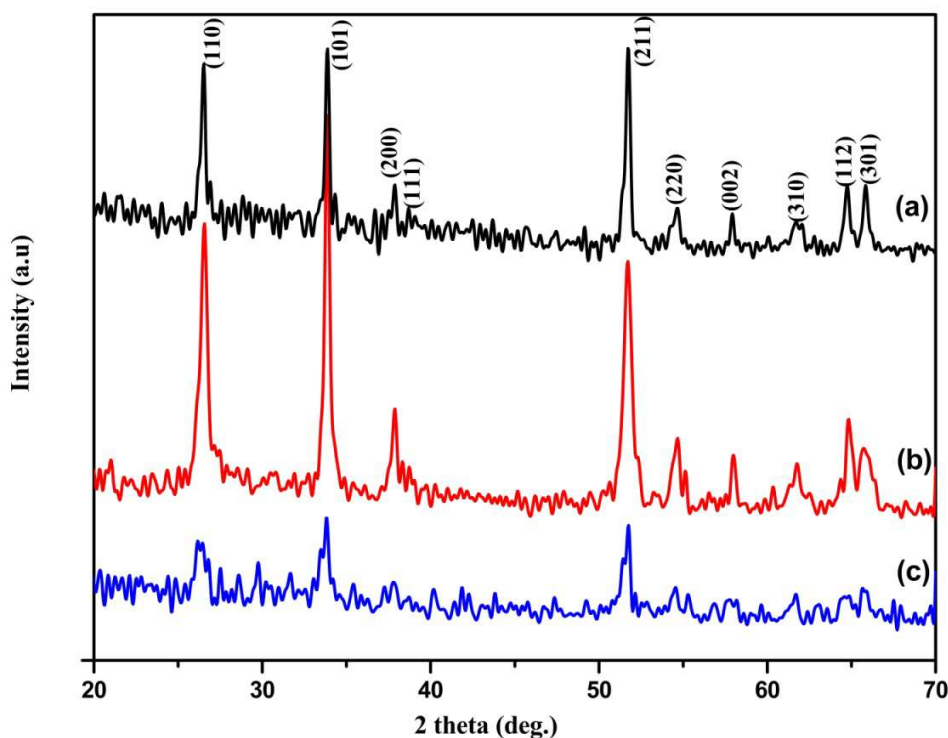


Fig. 1. X-ray diffraction patterns of SnO₂ nanostructures prepared with the assistance of (a) PEG 300 (b) PEG 400 and (c) PEG 600

3.2 FESEM analysis

The size and shape evolution of the as-prepared samples of SnO₂ as shown from the FESEM images (Fig. 2) reveal that there is a significant contribution of additive ligands with increasing chain length on the growth behavior of SnO₂. The synthesized products of tin oxide consist of flower-like nanoclusters of nanorods made up of self assembly of nanoparticles with uniformity in shape of the crystallites. The high magnification image (Fig. 2 b, d, f) further confirms that the nanorods have square shaped structure with sharp tips [19]. The average length was found to be around 1.11 μm , 379 nm and 347 nm whereas; the diameter of the nanorods was around 247 nm, 96 nm and 210 nm when molecular weight of PEG was varied as 300, 400 and 600 respectively. It is noteworthy to understand the effect of PEG molecular weights in controlling the morphology.

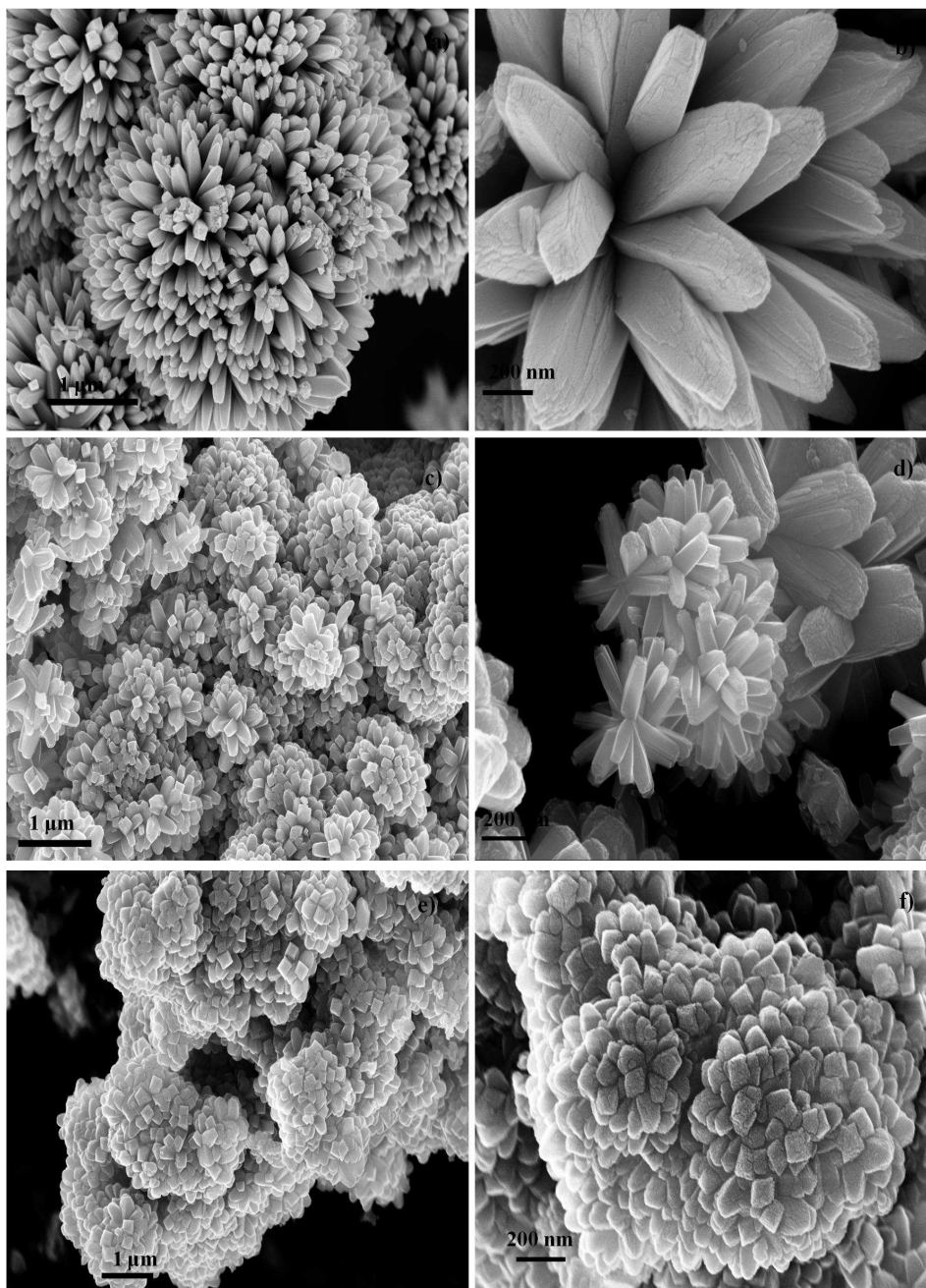


Fig. 2. FESEM images of flower-like SnO₂ nanorods prepared using PEG 300 (a, b), PEG 400 (c, d), and PEG 600 (e, f)

The experimental results suggest that when PEG ($M_w=300$) was used, the average diameter of the individual nanorod in flower-like nanostructures increased significantly when compared to the nanorods formed with PEGs of higher molecular weight ($M_w=400$ and 600). Uniformity in size and shape of the nanorods is evident for PEG 300, whereas suppression in the growth rate of the nanorods could be observed from the images of SnO₂ obtained from PEG 400. The suppression in growth of the nanorods is more vigorous for the sample prepared with PEG 600. However, homocentric growth was strictly maintained throughout the process and flower-like morphologies has been retained for all the three samples prepared with different molecular weight. These results clearly reveal that the size, aspect ratio and the uniformity in the flower-like nanorods are tunable by using PEG of varying molecular

weight. Cheng et al. used ethylenediamine as a structure directing template under solvothermal treatment at 220 °C for 25 h. When the volume ratio between the surfactant and water was tuned to 1:2, the obtained SnO₂ nanorods seemed to be organized into microrings [17]. But in the present case, when PEG is used as a structure directing agent with the same volume ratio of 1:2 with water, flower-like structures with uniform nanorods are formed. Moreover, no other morphologies were detected, reflecting the high yield of hierarchical structures [20]. It is possible to conclude that 100% morphological yield can be obtained when PEG 300 is used. Other important factor which governs the morphology of 1D SnO₂ nanostructure is the condition of pH. Only tiny spherical particles were formed at lower pH values. Hence in our case, the reaction was maintained at a pH of 12, to obtain uniform nanorods grown by oriented attachment process [6]. It is evident from the results of earlier work that hydrothermal temperature at 100 and 140 °C lead to the irregular agglomeration. Thus the ideal hydrothermal temperature would be 200 °C for the nuclei to grow in a controlled manner receiving more energy by absorbing the surrounding ones, resulting in the formation of homocentrally grown nanorods.

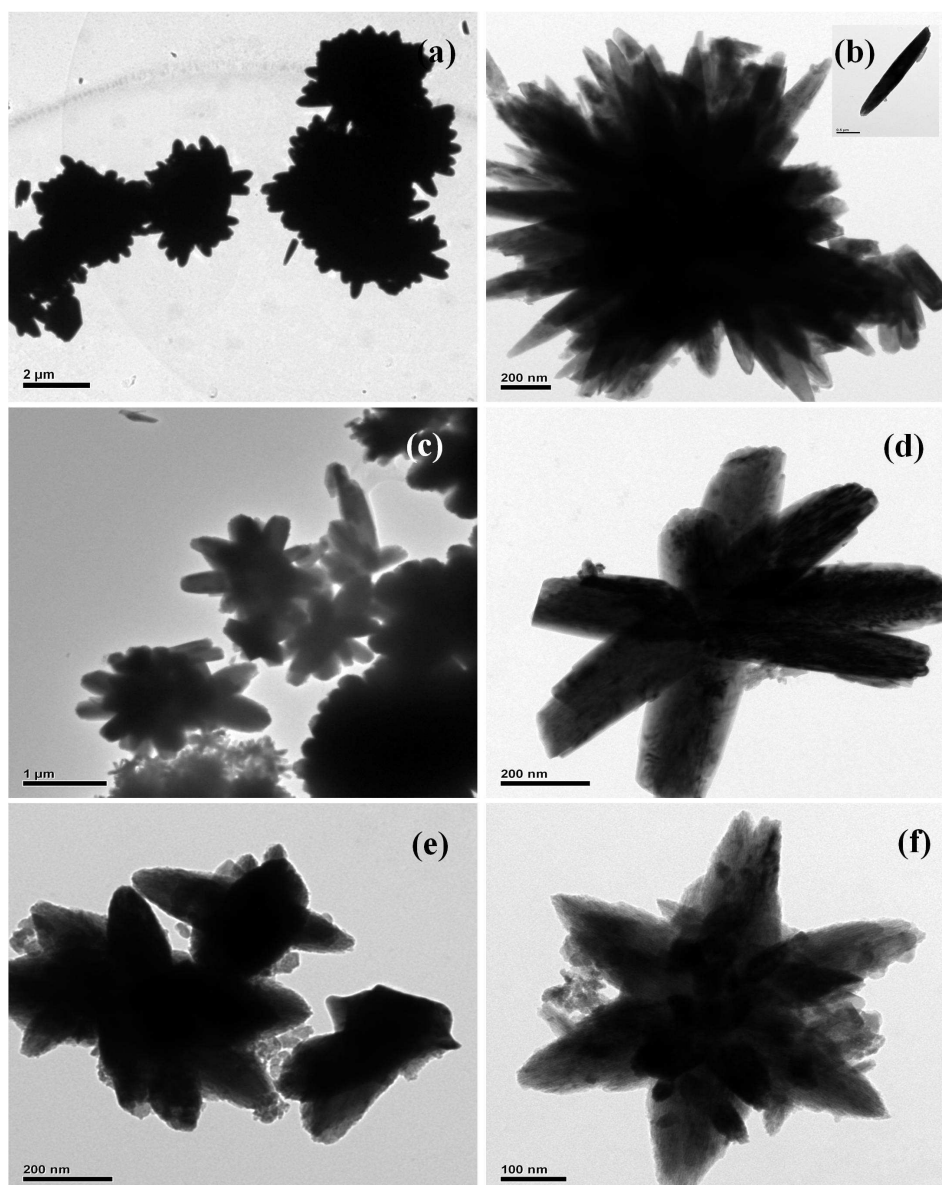


Fig. 3. TEM images of flower-like SnO₂ nanorods prepared using structure directing agent of PEG 300 (a, b - inset showing single nanorod), PEG 400 (c, d) and PEG 600 (e, f)

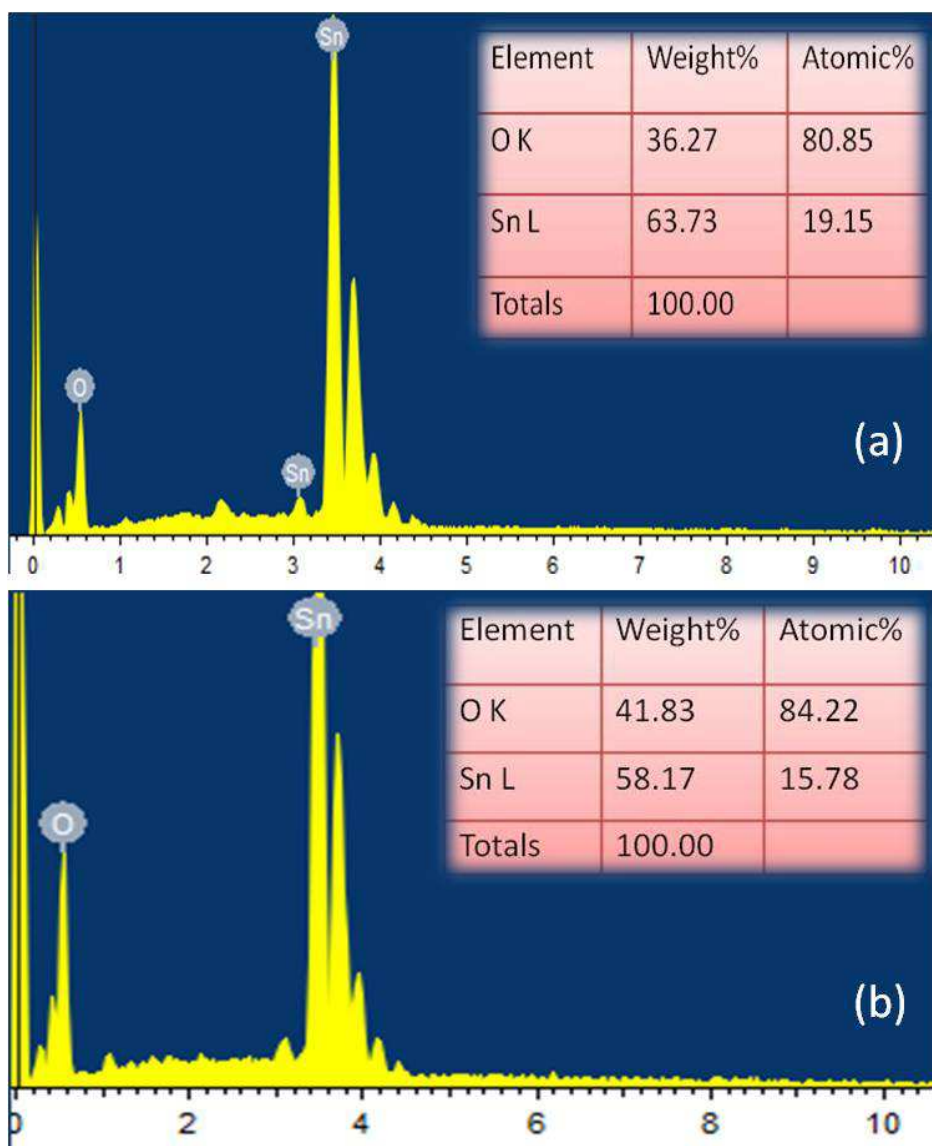
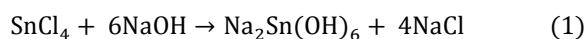


Fig. 4. EDX spectra of (a) PEG 300 and (b) PEG 400 assisted SnO₂ nanostructures

3.3 TEM analysis

Detailed investigations on the morphological features have also been obtained using TEM images. It is clearly evident from the images (Fig. 3 a-f) that the nanorods grow homocentrically and form flower-like structures. The orientation transformation takes place from nanoparticles to nanorods in which large quantities of SnO₂ nuclei tend to orient and aggregate to form thermodynamically stable nanorods [21]. The initially formed uniform SnO₂ nanoparticles under hydrothermal treatment tend to dissolve in the solution and grow as larger nanoparticles of SnO₂ to minimize the overall energy in the system [21, 22]. Later, these larger nanoparticles aggregate in to single crystalline nanorods. Thus the maximum reduction in the surface energy is supposed to be the driving force in the oriented aggregation course for the nanorod formation. The SnO₂ nanorods formed at 200 °C for all the three samples are found to have larger diameter due to the lower condensation among Na₂Sn(OH)₆ intermediate phases, reducing the growth rate at [001] direction which is in good agreement with the earlier reported work by Lipeng Qin et al. [19]. The proposed reaction process for the formation of SnO₂ nanocrystals can be illustrated as follows.





Similarly, it is worth to note that PEG plays a major role in determining the morphology of the product. Xiaoming Zhou et al. have reported that when PEG gets absorbed on the SnO_2 surface, the activities on some area of its surface will be changed [14]. In our work, the amount of PEG used in the solution is kept a constant and its influence has been investigated only by varying the molecular weights ($M_w = 300, 400, 600$). It is evident from the TEM images that the changes in PEG molecular weight have altered the texture of the obtained material.

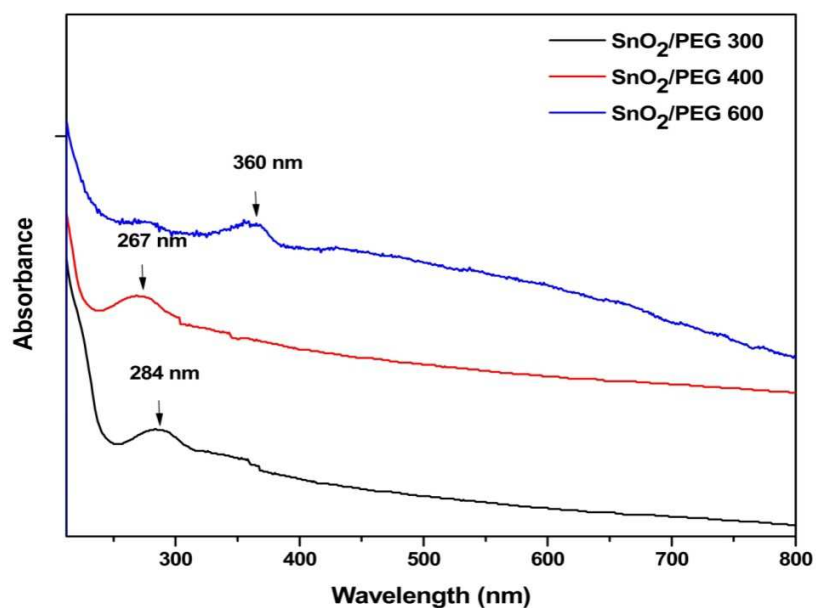


Fig. 5. UV-Vis absorption spectra of PEG assisted SnO_2 nanostructures

3.4 EDX spectral analysis

The EDX spectra of SnO_2 nanorods prepared with PEG 300 and 400 are shown in Fig. 4 (a,b), respectively. The spectra of both the samples reveal the presence of Sn and O as the only species in the nanopowder, indicating the purity of the synthesized samples. It is further evident that the samples exhibited Sn peaks with strong intensity than the O peaks and the composition of the samples in both atomic and weight percentage are tabulated in Fig. 4.

3.5 UV- vis spectral analysis

Optical absorbance spectra (Fig. 5) were recorded to investigate the size and shape dependent properties of 1D nanorod bundles. The maximum adsorption signals are located at 284 nm (4.3 eV), 267 nm (4.6 eV) and 360 nm (3.4 eV) for the SnO_2 samples prepared with PEG 300, 400 and 600, respectively. It could be observed that the absorption band exhibited a blue shift for the SnO_2 nanostructures assisted by PEG 300 and 400, whereas a red shift is noticed for the sample assisted with PEG 600. The PEG 400 directed sample showed a slightly higher shift than the SnO_2 sample prepared with PEG 300. Thus, it can be concluded that the origin of the blue shift is due to the decreasing size of the nanorods. The red shift in the PEG 600 assisted SnO_2 sample may be due to the suppression in the anisotropic growth of the nanorods. Also the crystalline imperfection is the largest for the nanorods prepared with PEG 600, which is also evident from the weak peak intensity of its XRD pattern.

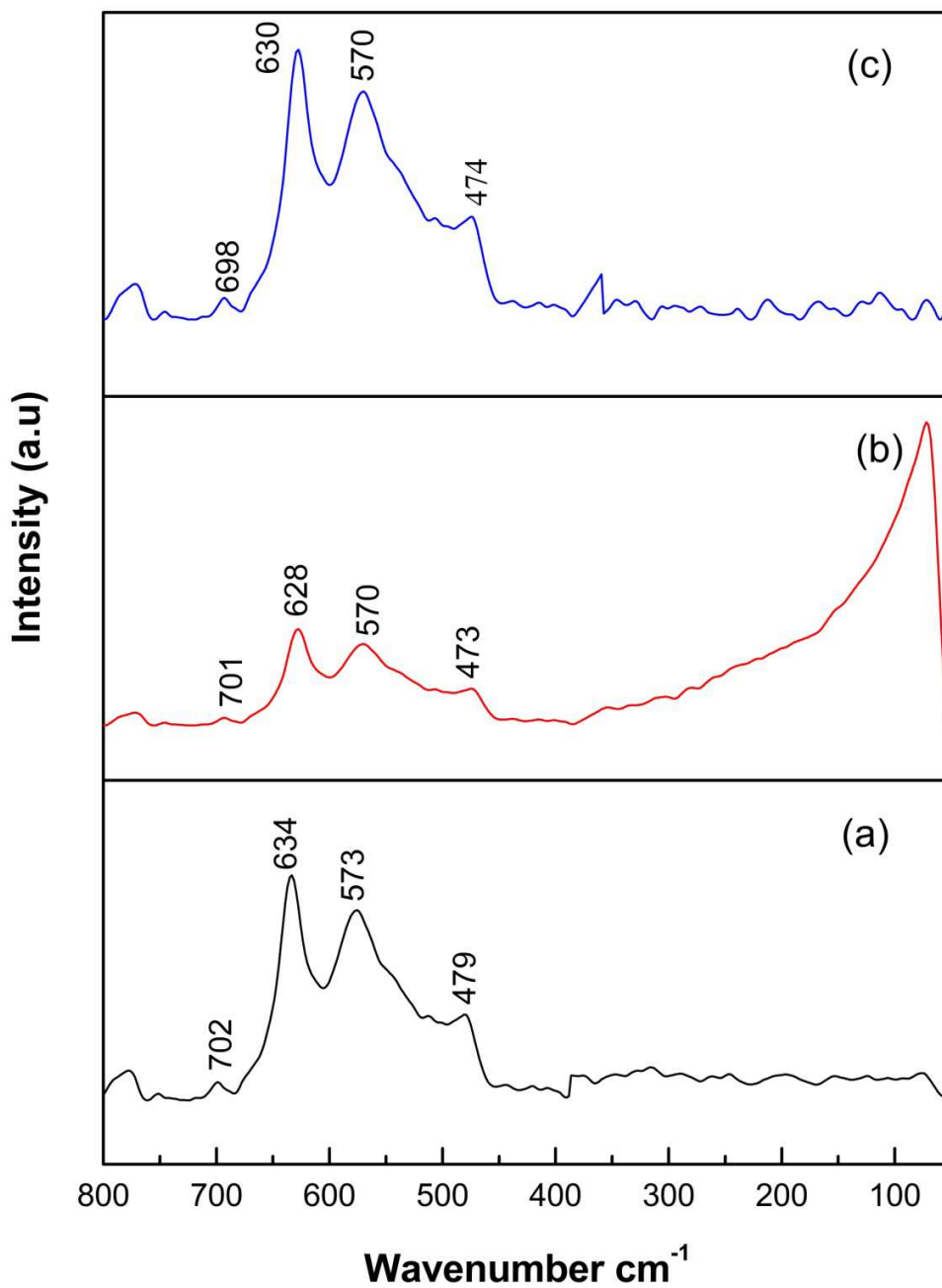


Fig. 6. FT-Raman spectra of (a) PEG 300 (b) PEG 400 and (c) PEG 600 assisted SnO₂ nanorods

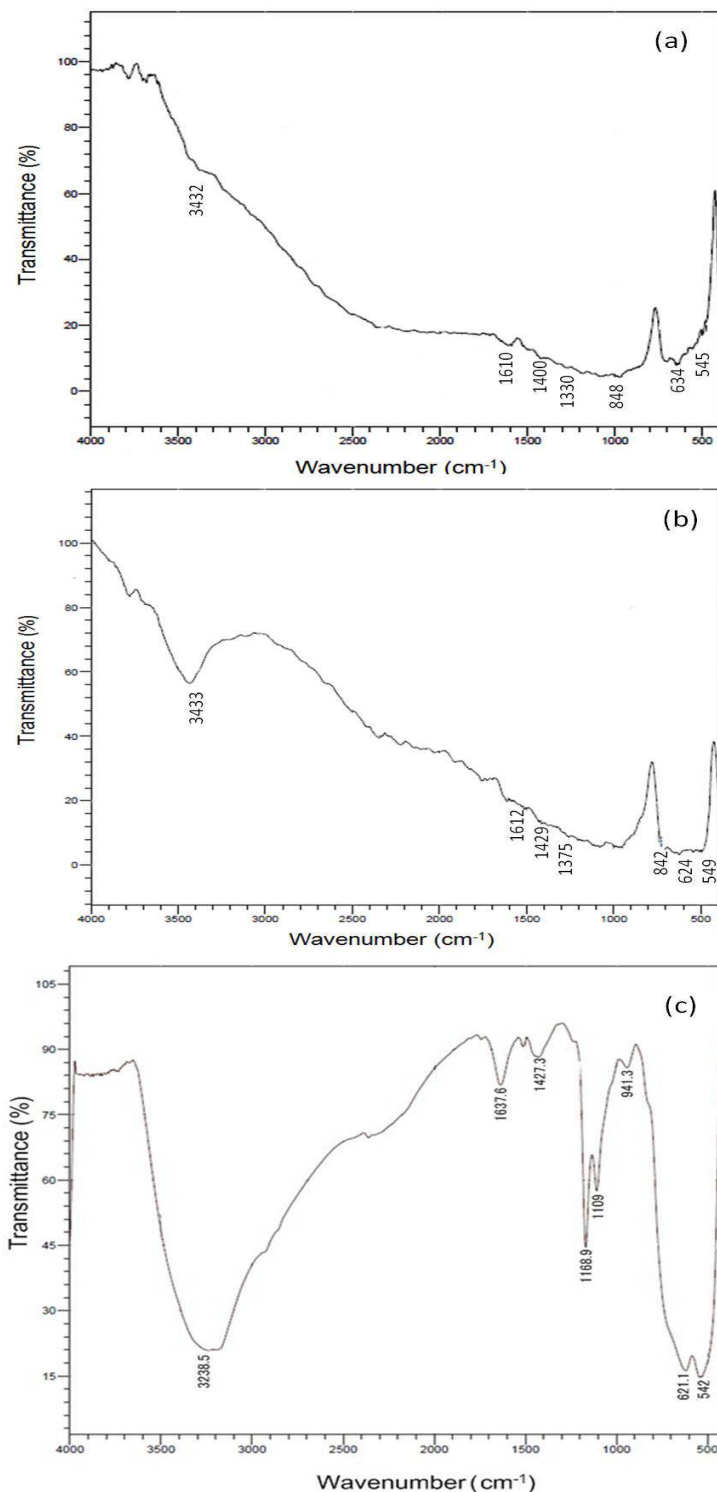


Fig. 7. FT-IR spectra of (a) PEG 300 (b) PEG 400 and (c) PEG 600 assisted SnO₂ nanorods

3.6 FT-Raman spectral analysis

Fig. 6 shows the FT-Raman spectra recorded for the three samples. The fundamental Raman scattering peaks for PEG 300 assisted SnO₂ sample appeared at about 479, 634 and 702 cm⁻¹ [23], whereas, for PEG 400 directed SnO₂ sample, peaks at 473, 628, and 701 cm⁻¹ are observed, which could be attributed to E_g, A_{1g}, B_{2g} modes, respectively.

Thus the shifts in the peak positions are obtained due to the size effect of the nanocrystalline SnO₂ particles and probable existence of tensile strength in the nanorods. Similar such trend was also attributed by Zhang et al. [5]. The origin of the strong and broad Raman peak at 570 cm⁻¹ in the PEG 300 and PEG 400 assisted SnO₂ nanorods is directly related to the surface structure and growth conditions rather than the crystallite size [24]. The appearance of unexpected new peaks established in the samples was due to the defects of nanocrystallites such as oxygen vacancies and vacancy clusters [17]. Therefore, the local lattice disorder at the interface and at the interior of the nanocrystal surface, generate these kinds of silent modes which were almost unrecognizable [6].

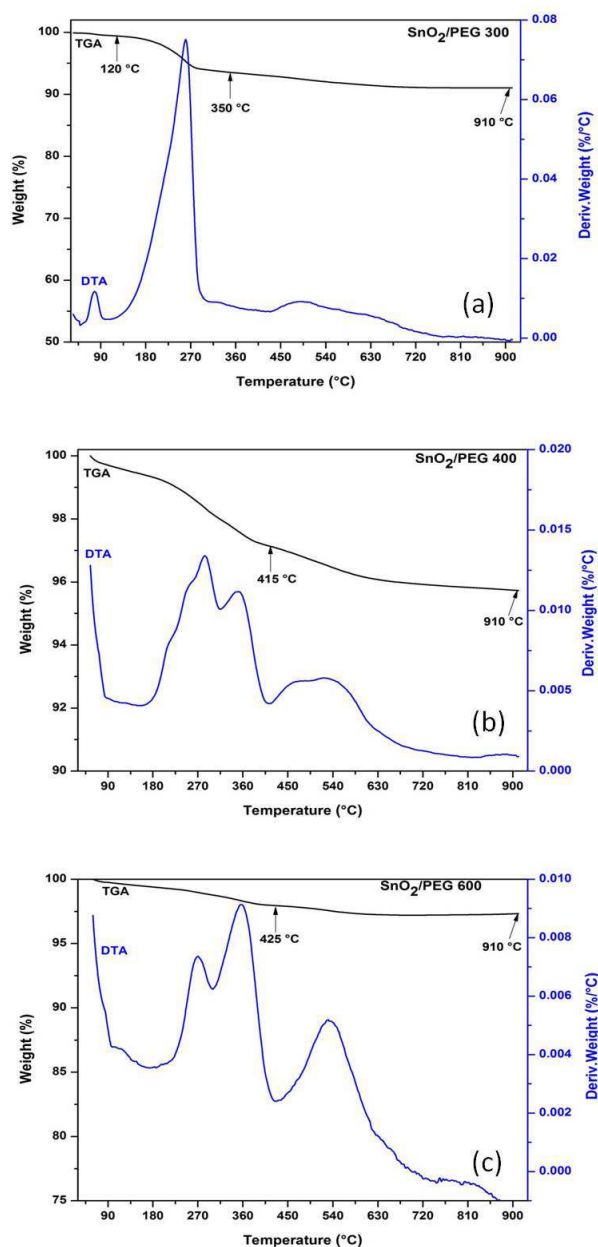


Fig. 8. TG and DTA curves of (a) PEG 300 (b) PEG 400 and (c) PEG 600 assisted SnO₂ nanorods

3.7 FT-IR spectral analysis

The FT-IR transmission spectra of SnO₂ nanorods synthesized using PEG 300 and PEG 400 are depicted in Fig 7. The peak assigned in the spectra of the samples around 545 and 630 cm⁻¹ are the two key bands related to O-Sn-O and Sn-O stretching vibrations. The bending modes of different types of surface terminated -OH bands appear in the range of 848-1330 cm⁻¹, and 842-1375 cm⁻¹ for PEG 300 and PEG 400 directed SnO₂ samples, respectively [3]. The peaks observed around 1610 and 3432 cm⁻¹ were attributed to the bending vibrations of residual water molecules or hydroxide groups adsorbed at the surface of the tin oxide [3]. The peak around 1400 cm⁻¹ is assigned to the C-H stretching and bending vibrations [25]. The FT-IR spectra of the three samples exhibit slight variations in the peak positions. These variations are caused not only due to size variations in these samples but also due to different stoichiometry as evident from the EDX result.

3.8 Surface area analysis

The BET surface areas of the PEG 300, 400 and 600 assisted SnO₂ samples were found to be 1.56 m²/g, 1.05 m²/g, 1.74 m²/g, respectively. The low surface area could be partly related to the attribution of SnO₂ with high density, as well as to the nanorods with larger diameter which acted as a building block of the hierarchical structures [1].

3.9 Thermal analysis

Fig. 8 illustrates the thermogravimetric analysis curve for the three samples obtained at 200 °C, under hydrothermal treatment using PEG of three different molecular weights. The minor weight loss found around 120 °C in all the three samples can be attributed to the dehydration of water molecules dissociatively adsorbed onto the surface of the tin oxide crystallites. The samples have also experienced a major weight loss in the temperature range from 350 °C to 425 °C. This reduction in the weight can be attributed to the evaporation of hydrated water molecule (SnO₂.nH₂O) [26, 18]. The total weight loss values are 4.94%, 3.26 % and 2.68 % for PEG 300, 400 and 600 assisted SnO₂ samples, respectively. Notably, only < 5% reduction in the total weight is observed in the entire TG-DTA curve, strongly indicating the purity and stability of the as-prepared samples.

CONCLUSION

In summary, our study demonstrates that the size, aspect ratio and uniformity of flower-like SnO₂ nanorod bundles are tunable by employing PEG of appropriate molecular weight as a structure directing agent via a cost effective solvothermal approach. Interestingly, when PEG 300 is used, 100% morphological yield with uniformity in size and shape is evident. However, with PEG of higher molecular weight, suppression in the growth rate of the nanorods is observed. FESEM study reveals that the change in the texture of the samples is influenced by variation of the PEG molecular weight. TEM result indicates that orientation attachment process is responsible for the formation of nanorods. The absorption spectra of the samples showed particle size-dependent shifts. Further, the result from Raman spectra supports the composition and single crystalline rutile structure of the sample. Based on the approach used and from the results obtained it can be concluded that it is highly possible to modify the properties and morphologies of SnO₂ nanoparticles by optimizing the molecular weight of PEG along with other low temperature experimental conditions.

Acknowledgement

The authors acknowledge Loyola College-Times of India (LC-TOI) Research initiative (Ref.No.3LCTOI14PHY001) for funding this research work and for providing the research facility at Department of Physics, Loyola College (Autonomous), Chennai -600034. We also thank Mr. Arul Maximus Rabel, Scientist, Centre for Nanoscience and Nanotechnology and Dr. Joseph Arul Pragasam, Professor of Physics, Sathyabama University for FESEM facility and for fruitful discussions.

REFERENCES

- [1] H B Wu, J S Chen, X W (David) Lou, H H Hng, *J. Phys. Chem. C*, **2011**, 115, 24605–24610.
- [2] A A Firooz, A R Mahjoub, A A Khodadadi, *Mater. Lett.*, **2008**, 62, 1789–1796.
- [3] S Das, S Kar, S Chaudhuri, *J. Appl. Phys.*, **2006**, 99, 114303 (1-7).
- [4] Z Zhang, J Gao, L M Wong, J G Tao, L Liao, Z Zheng, G Z Xing, H Y Peng, T Yu, Z X Shen, C H A Huan, S J Wang, T Wu, *Nanotechnology*, **2009**, 20, 135605 – 135615.
- [5] U Pal, M Pal, R S Zeferino, *J. Nanopart. Res.*, **2012**, 14, 1-10.
- [6] S Das, S Chaudhuri, S Maji, *J. Phys. Chem. C*, **2008**, 112, 6213-6219.

-
- [7] G E Patil, D D Kajale, S D Shinde, V B Gaikwad, G H Jain, *Int. Nano Lett*, **2012**, 2, 46-51.
- [8] G Cheng, K Wu, P Zhao, Y Cheng, X He, K Huang, *J. Cryst. Growth*, **2007**, 309, 53-59.
- [9] L Tan, L Wang, Y Wang, *J. Nano Mat*, **2011**, pp. 1-10.
- [10] Y J Chen, X Y Xue, Y G Wang, T H Wang, *Appl. Phys. Lett*, **2005**, 8, 233503 (1-3).
- [11] F Han, J Zhang, G Chen, X Wei, *J. Chem. Eng. Data*, 53 **2008**, 2598-2601.
- [12] Y X Yin, L Y Jiang, L J Wan, C J Li, Y G Guo, *Nanoscale*, **2011**, 3, 1802 – 1806.
- [13] X Zhou, W Fu, H Yang, D Ma, J Cao, Y Leng, J Guo, Y Zhang, Y Sui, W Zhao, M Li, *Mater. Chem. Phys*, **2010**, 124, 614–618.
- [14] Y J Chen, L Nie, X Y Xue, Y G Wang, T H Wang, *Appl. Phys. Lett*, **2006**, 88, 083105.
- [15] H Huang, S Tian, J Xu, Z Xie, D Zeng, D Chen, G Shen, *Nanotechnology*, **2012**, 23, 105502 (8pp).
- [16] G Cheng, K Wu, P Zhao, Y Cheng, X He, K Huang, *Nanotechnology*, **2007**, 18, 355604 (7pp).
- [17] Y Liang, B Fang, *Mater. Res. Bull*, **2013**, 48, 4118–4124.
- [18] L Qin, J Xu, X Dong, Q Pan, Z Cheng, Q Xiang, F Li, *Nanotechnology*, **2008**, 19, 185705 (8pp).
- [19] P Sun, L You, Y Sun, N Chen, X Li, H Sun, J Ma, G Lu, *Cryst. Eng. Comm*, **2012**, 14, 1701–1708.
- [20] G C Xi, J Ye, *Inorg. Chem*, **2010**, 49, 2302–2309.
- [21] D F Zhang, L D Sun, J L Yin, C H Yan, *Adv. Mater*, **2003**, 15, 1022-1025.
- [22] F Gu, S Wang, H Cao, C Li, *Nanotechnology*, **2008**, 19, 095708 (1-5)
- [23] K Sato, Y Yokoyama, J C Valmalette, K Kuruma, H Abe, T Takarada, *Cryst. Growth Des*, **2013**, 13, 1685-1693.
- [24] M A Farrukh, B T Heng, R Adnan, *Turk. J. Chem*, **2010**, 34, 537–550.
- [25] N S Baik, G Sakai, N Miura, N Yamazoe, *J. Am. Ceram. Soc*, **2000**, 83, 2983–2987.